Backward Echo in Two-Level Systems

M. Fujita, H. Nakatsuka, H. Nakanishi, and M. Matsuoka
Department of Physics, Faculty of Science, Kyoto University, Kyoto 606, Japan
(Received 12 February 1979)

The possible three-pulse echoes in two-level systems of solids and gases are discussed with particular emphasis on backward-wave echoes. One example of the backward echoes was realized with the atomic sodium D line. The detection of this echo requires neither optical shutters nor magnetic field. The decay rate of the echo due to Na-Ar collisions was measured. It is shown that the effect of velocity changing collisions is negligible compared with that of phase interrupting ones.

We have observed a new photon echo in a two-level system, a backward-wave three-pulse echo in a gas. This is unique to the optical frequency domain. In this method neither optical shutters[1,2] nor magnetic field[3] is required to prevent the excitation pulses from saturating a detector.

In the first observation of the photon echo in ruby,[1] a Kerr-cell shutter was placed before a phototube, and noncollinear (~ 50 mrad) first and second pulses were used at the sacrifice of a phase-matching condition. Later[2] a series of three Pockels cells was used which provided more than 10^9 extinction ratio. In the category of the echoes by pulsed lasers, apart from the Stark or frequency-switching method,[4] a weak axial magnetic field was used[3] to separate the echo by rotation of the echo polarization. In a three-level system, a backward echo was observed using two different frequencies (trilevel echo).[5]

In the present experiment, a phase-matching condition is satisfied in the configuration in which the three excitation pulses and the echo, all of a same frequency, are counterpropagating or making angles with each other. As a result of this configuration, the echo can be polarized perpendicularly to one of the excitation pulses which makes the smallest angle to the echo. This method allows a simple and very easy detection of the echo compared with the previous method, together with some new possibilities for application. We have observed this echo in Na on the $3^2S_{1/2}$-$3^2P_{1/2}$ two-level system.

We apply the ordinary two-pulse echo theory by Scully, Stephen, and Burnham[5] to general three-pulse echoes. Suppose the three excitation pulses are applied at times τ_p ($p = 1$, 2, and 3) in the directions along unit vectors $\hat{n}_p$. (We will set $\tau_1 = 0$ in the following.) The arrival times t_{pi} at the ith atom at the position $\vec{r}_i(t_{pi})$ are determined by the equations

$$ct_{pi} = c\tau_p + \hat{n}_p \cdot \vec{r}_i(t_{pi}). \tag{1}$$

With respect to an observation time t and position $\vec{R} = R\hat{n}$, where $\hat{n}$ is a unit vector, we define the retarded time t_i as

$$ct_i = ct - R + \hat{n} \cdot \vec{r}_i(t_i). \tag{2}$$

Then the state of the ith atom at t_i is expressed by a density operator

$$\rho_i(t_i) = \exp[-iH_{0i}(t_i - t_{3i})]U_3 \exp[-iH_{0i}(t_{3i} - t_{2i})]U_2 \exp[-iH_{0i}(t_{2i} - t_{1i})]U_1\rho_0 \times U_1^\dagger \exp[iH_{0i}(t_{2i} - t_{1i})]U_2^\dagger \exp[iH_{0i}(t_{3i} - t_{2i})]U_3^\dagger \exp[iH_{0i}(t_i - t_{3i})], \tag{3}$$

where ρ_0 is the density operator of the ground state, H_{0i} the Hamiltonian of the ith atom, and U_p a transformation operator expressing the effect of the pth pulse.

If we express the ground and the excited levels as a and b, respectively, the effect of the transformations U_p which leads to the echo component ρ_{ba} is as follows. The first pulse transforms the ground state into [A] ρ_{ab} or [B] ρ_{ba}, each of which has the phase factor $\exp[+i\omega_i(t_{2i} - t_{1i})]$ or $\exp[-i\omega_i(t_{2i} - t_{1i})]$ at the time t_{2i}, where ω_i is the eigenfrequency of the ith atom. The second pulse transforms them into diagonal elements ρ_{bb} or ρ_{aa}. The third pulse transforms ρ_{bb} and ρ_{aa} into ρ_{ba}, which gets an additional phase factor $\exp[-i\omega_i(t_i - t_{3i})]$ at the time t_i. Depending on the paths [A] or [B], we have two terms for the polarization as in the following:

$$\langle P_i(t_i)\rangle_{\text{echo}} = \{\alpha \sin\theta_1 \sin\theta_2 \sin\theta_3 \exp[-i\omega_i(t_i + t_{1i} - t_{2i} - t_{3i})] + \text{c.c.}\} + \{\beta \sin\theta_1 \sin\theta_2 \sin\theta_3 \exp[-i\omega_i(t_i - t_{1i} + t_{2i} - t_{3i})] + \text{c.c.}\}, \tag{4}$$

where the first pair of braces sets off the terms for path [A] and the second those for path [B], and where θ_p is the area of the pth pulse (α and β are constants). When the velocity $\vec{v}_i$ of the ith atom is constant, $\vec{r}_i(t)$ is given by

$$\vec{r}_i(t) = \vec{r}_i(0) + \vec{v}_i t. \tag{5}$$

The radiated field at $\vec{R}$ and t is given by

$$E(\vec{R},t) \propto \sum_i \langle P_i(t_i)\rangle_{\text{echo}}, \tag{6}$$

which leads to

$$\begin{aligned} E(\vec{R},t) \propto &\Big\{\sum_i \alpha \sin\theta_1 \sin\theta_2 \sin\theta_3 \exp\Big[-i\omega_i\{(t-R/c-\tau_2-\tau_3)+(\vec{r}_i/c)(\hat{n}+\hat{n}_1-\hat{n}_2-\hat{n}_3) \\ &+(\vec{v}_i/c)[(t-R/c)\hat{n}-\tau_2\hat{n}_2-\tau_3\hat{n}_3]+O(\vec{r}_i\cdot\vec{v}_i/c^2)\}\Big]+\text{c.c.}\Big\} \\ &+\Big\{\sum_i \beta \sin\theta_1 \sin\theta_2 \sin\theta_3 \exp\Big[-i\omega_i\{t-R/c+\tau_2-\tau_3)+(\vec{r}_i/c)(\hat{n}-\hat{n}_1+\hat{n}_2-\hat{n}_3) \\ &+(\vec{v}_i/c)[(t-R/c)\hat{n}+\tau_2\hat{n}_2-\tau_3\hat{n}_3]+O(\vec{r}_i\cdot\vec{v}_i/c^2)\}\Big]+\text{c.c.}\Big\}, \end{aligned} \tag{7}$$

where again the separation into paths [A] and [B] is indicated by (oversize) braces.

First, we discuss the [A] term of Eq. (7).

(i) In a solid, $\vec{v}_i = 0$, but there is an inhomogeous broadening in ω_i, and so the condition on which all atoms have the same phase to form an echo are as follows:

$$t - R/c = \tau_2 + \tau_3, \tag{8a}$$

$$\hat{n} + \hat{n}_1 - \hat{n}_2 - \hat{n}_3 = 0. \tag{8b}$$

Equation (8a) gives the echo time. The phase-matching condition (8b) allows three different configurations, Figs. 1(a)–1(c) where we assume for simplicity that all the vectors are in a plane, but generally this condition is not required. The angle θ here is arbitrary. Figures 1(a) and 1(b) reduce to the ordinary stimulated echo when $\theta \cong 0$. The case 1(c) is the one to generate a backward echo, and the echo is the delayed, phase-conjugated image wave of the first pulse. This has already been proposed by Shiren.[6]

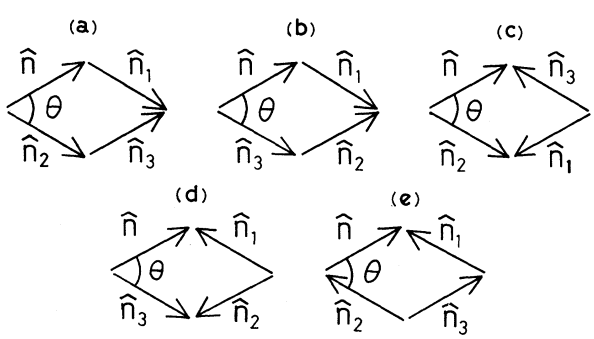

FIG. 1. The possible configurations of the propagation vectors $\omega\hat{n}_1/c$, $\omega\hat{n}_2/c$, and $\omega\hat{n}_3/c$ of the three excitation pulses and $\omega\hat{n}/c$ of the echo. They are assumed to be coplanar.

(ii) In a gas, $\omega_i = \omega$ for all atoms, but there is a spread in $\vec{v}_i$; hence the conditions for the echo formation are given by

$$\hat{n} + \hat{n}_1 - \hat{n}_2 - \hat{n}_3 = 0, \tag{9a}$$

$$(t - R/c)\hat{n} = \tau_2\hat{n}_2 + \tau_3\hat{n}_3. \tag{9b}$$

Taking the inner product of $\hat{n}$ and Eq. (9b), we have

$$t - R/c = \tau_2\hat{n}\cdot\hat{n}_2 + \tau_3\hat{n}\cdot\hat{n}_3. \tag{9c}$$

Equations (9a) and (9b) have two cases, shown in Figs. 1(a) and 1(b), where the angle θ should be smaller than 90° because of Eq. (9c) and the condition $t - R/c > \tau_3$. When $\theta \neq 0$, Eq. (9b) is not completely satisfied, and therefore perfect rephasing does not occur. We can evaluate the echo amplitude $E(\vec{R},t)$ and find

$$E(\vec{R},t) \propto \langle \exp\{-i(\omega/c)\vec{v}_i(\tau_2\vec{n}_{2\perp} + \tau_3\vec{n}_{3\perp})\}\rangle_i = \exp\{-[\tfrac{1}{2}(\omega/c)u\tau\sin\theta]^2\}, \tag{10}$$

where $\vec{n}_{p\perp} = \hat{n}_p - \hat{n}(\hat{n}_p\cdot\hat{n})$, and $\tau = \tau_2$ in 1(a) and $\tau = \tau_3$ in 1(b), and u is the most probable speed of the atom.

Next, we go to the [B] term of Eq. (7). (i) In a solid, the condition for the echo given by

$$(t - R/c) - \tau_3 = -\tau_2$$

implies that no echo should appear. (ii) In a gas, the conditions are given by

$$\hat{n} - \hat{n}_1 + \hat{n}_2 - \hat{n}_3 = 0, \tag{11a}$$

$$(t - R/c)\hat{n} = \tau_3\hat{n}_3 - \tau_2\hat{n}_2. \tag{11b}$$

From Eq. (11b) we get

$$t - R/c = \tau_3\hat{n}_3\cdot\hat{n} - \tau_2\hat{n}_2\cdot\hat{n}. \tag{11c}$$

Equations (11a) and (11b) allow the two cases

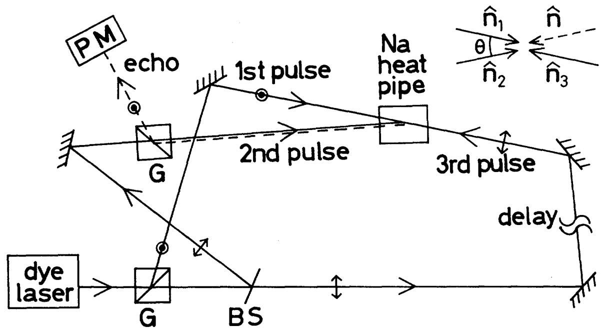

FIG. 2. Experimental setup for the backward echo on the Na D line, corresponding to Fig. 1(d). G, Glan prism; BS, beamsplitter; PM, photomultiplier. The polarization of each beam is indicated.

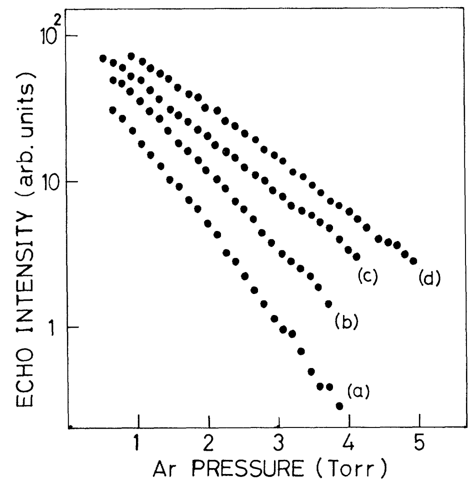

FIG. 3. Measured echo intensity as a function of Ar pressure for four pairs of τ_2 and τ_3: curve a, $\tau_2=6.6$ nsec and $\tau_3=11.0$ nsec; curve b, $\tau_2=4.9$ nsec and $\tau_3=10.9$ nsec; curve c, $\tau_2=3.5$ nsec and $\tau_3=17.2$ nsec; curve d, $\tau_2=3.5$ nsec and $\tau_3=7.9$ nsec. Each point represents an average of about fifty laser shots. The relative intensities for curves a–d are arbitrary.

shown in Figs. 1(d) and 1(e), and (11c) requires $\theta<90°$. The echo amplitude has the same θ dependence as Eq. (10), where in 1(d) $\tau=\tau_3$, and in 1(e) $\tau=\tau_2$. The backward echo is realized in 1(d), and for small θ in 1(e). In 1(d), the echo is the delayed, phase-conjugated image wave of the second pulse.

In our experiment, we used the geometry of Fig. 1(d). The experimental setup is quite simple as is shown in Fig. 2. A nitrogen-laser pumped dye laser produced 2-nsec-long, 1-kW pulses at 5896 Å with a spectral width of 0.5 cm^{-1}. The polarizations of the excitation pulses and the echo are shown in Fig. 2. These excitation pulses irradiated the Na vapor in a 30-cm-long heat pipe with Ar buffer gas. The hot region of the heat pipe was about 3 cm long. We chose the angle θ between the first and the second pulse to be ~20 mrad, and made the polarization of the echo perpendicular to that of the third pulse. In this way we have easily separated the echo from the excitation pulses. In the low-pressure limit of Ar gas, the intensity of the echo was two orders of magnitude larger than that of the scattered excitation pulses at the detector.

We studied the decay of the echo due to Na-Ar collisions. By collisions, $\vec{v}_i(t)$ and $\omega_i(t)$ may change, and $\vec{r}_i(t)$ and $\omega_i(t)$ are given by

$$\vec{r}_i(t)=\vec{r}_i(0)+\int_0^t \vec{v}_i(t')\,dt', \tag{12}$$

$$\omega_i(t)=\omega+\Delta\omega_i(t), \tag{13}$$

in the classical limit. With $\theta=0$ in Fig. 1(d),

$$E(\vec{R},t)\propto\langle\exp\{-i[\int_0^{\tau_2}\Delta\omega_i(t')\,dt'+\int_{\tau_3}^{t-R/c}\Delta\omega_i(t')\,dt']+(i\omega/c)[\int_0^{\tau_2}\hat{n}\cdot\vec{v}_i(t')\,dt'-\int_{\tau_3}^{t-R/c}\hat{n}\cdot\vec{v}_i(t')\,dt']\}\rangle_i \times\exp[-\Gamma(t-R/c+\tau_3-\tau_2)], \tag{14}$$

where Γ is the spontaneous emission rate of the excited level. The first term in the curly brace represents the effect of phase-interrupting collisions, and the second term is that of velocity-changing collisions. It must be noted that between the second and the third pulse, only the velocity-changing collisions affect the echo amplitude. From this fact we can separate these two effects in our experiment. This is not possible in the ordinary two-pulse echoes.

For several pairs of τ_2 and τ_3, we have measured the echo intensity as a function of the Ar buffer-gas pressure. The data at a temperature of 420°K are shown in Fig. 3. Each point represents an average of about 50 laser shots. This figure shows that the echo intensity behaves as $I=I_0e^{-\beta p}$, where p is the Ar pressure. At higher temperatures, the values of β decreased with temperature. We attributed this to the reabsorption of the echo. But we have checked that this effect is negligible around 420°K.

From curves c and d in Fig. 3, we see that β is equal for the same τ_2 but different τ_3. This means that the effect of the velocity-changing collisions is too small to be observed with our experimental accuracy. We find that $\gamma = \tau_2/\beta = 4.1 \pm 0.3$ nsec Torr, which agrees well with the result of Ref. 2. Here we have used τ_2, because the collisions give no effect on the decay of the echo between the second and the third pulse.

At this point we want to make a remark about the relationship between our backward three-pulse echo and the trilevel echo by Mossberg *et al.*[7] The former may be considered as a two-level version of the latter in the sense that the third and ground levels are degenerate.

We have discussed the general case of three-pulse echoes on two-level systems in solids and gases. One example of the backward echoes has been demonstrated on the Na *D* line with a simple experimental setup. In this study, it is shown that in Na-Ar collisions the velocity-changing collisions are negligible compared with the phase-interrupting ones. Finally, we point out several advantages of backward echoes: (i) easy elimination of excitation pulses, (ii) applicability to the picosecond regime, and (iii) wide range of applicability to the problems of two-level systems from solids to gases.

[1]N. A. Kurnit, I. D. Abella, and S. R. Hartmann, Phys. Rev. Lett. 13, 567 (1964); I. D. Abella, N. A. Kurnit, and S. R. Hartmann, Phys. Rev. 141, 391 (1966).

[2]A. Flusberg, T. Mossberg, and S. R. Hartmann, Opt. Commun. 24, 207 (1978).

[3]T. Baer and I. D. Abella, Phys. Rev. A 16, 2093 (1977).

[4]R. G. Brewer and R. L. Shoemaker, Phys. Rev. Lett. 27, 631 (1971); R. G. Brewer and A. Z. Genack, Phys. Rev. Lett. 36, 959 (1976).

[5]M. Scully, M. J. Stephen, and D. C. Burnham, Phys. Rev. 171, 213 (1968).

[6]N. S. Shiren, Appl. Phys. Lett. 33, 299 (1978). He discussed Fig. 1(c) of the [A] term, and concluded that the backward echo could not be formed in a gas.

[7]T. Mossberg, A. Flusberg, R. Kachru, and S. R. Hartmann, Phys. Rev. Lett. 39, 1523 (1977).

High-Power, cw, Efficient, Tunable (uv through ir) Free-Electron Laser Using Low-Energy Electron Beams

Luis R. Elias

Department of Physics and High Energy Physics Laboratory, Stanford University, Stanford, California 94305

(Received 16 January 1979)

Using beams of low-energy electrons ($E < 5$ MeV), a free-electron laser can be operated as a continuously tunable (1000 Å $< \lambda <$ 50 μm), high-power ($P > 10$ kW, cw) source of laser radiation. With electrostatic accelerators the electron beam can be recycled to increase the overall efficiency of the laser. Wall power to laser power efficiencies greater than 10% are possible.

The amplification of optical radiation by a beam of relativistic electrons moving through a static, spatially periodic transverse magnetic field, proposed by Madey in 1971,[1] was demonstrated by Elias *et al.*[2] In 1977 Deacon *et al.*[3] reported the operation of the free-electron laser (FEL), above threshold, as an optical oscillator at a wavelength of 3.4 μm.

Lasers based on the technique used in these Stanford experiments are important because they have the potential capability of operating as sources of optical radiation with the following highly desirable characteristics[4]: (a) high average output power, (b) broadband continuous wavelength tunability, (c) high optical resolution, and (d) very high overall efficiency.

The prospect for high-power operation stems from the experimental result[3] that nearly 0.2% of the electron kinetic energy can be converted to optical radiation. Characteristic (b) arises, principally, from the dependence of wavelength on electron energy. The range of energies available from present electron accelerators is quite large. Laser operation can thus be obtained at wavelengths anywhere between 1 mm and 1000 Å. Characteristic (c) stems from the observed ability of the FEL to radiate a homogeneously broadened spontaneous spectrum.

The capability (d) of operating the FEL at high overall efficiency has received considerable recent attention. As was noted earlier, in the Stanford experiments, a maximum of 0.2% of the elec-